Average density of states in disordered graphene systems

Shangduan Wu,[1,2] Lei Jing,[1,2] Qunxiang Li,[1] Q. W. Shi,[1,*] Jie Chen,[3,4] Haibin Su,[5] Xiaoping Wang,[1] and Jinlong Yang[1]
[1]*Hefei National Laboratory for Physical Sciences at Microscale, University of Science and Technology of China, Hefei, Anhui 230026, People's Republic of China*
[2]*Department of Physics, University of Science and Technology of China, Hefei, Anhui 230026, People's Republic of China*
[3]*Electrical and Computer Engineering, University of Alberta, Alberta, Canada T6G 2V4*
[4]*National Institute for Nanotechnology, Edmonton, Alberta, Canada T6G 2M9*
[5]*Division of Materials Science, Nanyang Technological University, 50 Nanyang Avenue, 639798 Singapore, Singapore*
(Received 17 January 2008; revised manuscript received 1 April 2008; published 8 May 2008; corrected 2 June 2008)

In this paper, the average density of states (ADOS) in graphene with binary alloy disorders is calculated by the recursion method. We observed an obvious resonant peak and a dip in ADOS curves near the Dirac point, which result from interactions with surrounding impurities. We also found that the resonance energy (E_r) and the dip position (ε_{dip}) are strongly dependent on the concentration of disorders (x) and their on-site potentials (v). A linear relation, $\varepsilon_{\text{dip}}=xv$, holds when the impurity concentration is low. This relation can also be extended when the impurity concentration is high, but with certain constraints. We also compute ADOS with a finite density of vacancies.

DOI: 10.1103/PhysRevB.77.195411 PACS number(s): 81.05.Uw, 71.55.−i, 71.23.−k

I. INTRODUCTION

Graphene is a two-dimensional material with a single atomic layer of graphite. The material was initially fabricated by rubbing graphite layers against an oxidized silicon surface.[1] Due to the linear dispersion relation of its electronic spectrum near the Dirac point, the electron transport behavior of graphene at low-energy range is essentially determined by the massless relativistic Dirac equations. Many interesting properties of graphene have been experimentally studied. The key physical properties include the unusual quantum Hall effect,[2–4] minimal conductivity,[4–10] ferromagnetism,[11,12] and superconductivity.[13–15]

Disorders in graphene can significantly impact their electronic properties, which have been extensively studied over the past decades.[12,16–27] The interplay between disorders and electron-electron interactions determines the low-energy behavior of electrons in graphene.[4] Due to the disorder, the average density of states (ADOS) increases near the Dirac point. The minimum conductivity (σ_{min}) can be estimated through the Einstein relation ($\sigma_{\text{min}}=\rho D$) by calculating the diffusion constant (D) and ADOS (ρ) at the Dirac point. To date, various methods have been proposed to calculate ADOS and the local density of states (LDOS) in various types of disorders in graphene, such as Anderson disorder,[28,29] short-range potential disorder,[10,30–34] long-range potential disorder,[10] and atomic vacancies.[4,35] However, these calculated results are unreliable due to limitations in the approximations used. These calculations are only suitable for addressing an electronic structure with a low impurity concentration. It is, therefore, important to explore robust schemes to accurately describe the electronic structure of the disordered graphene.

Recently, the phenomenon of spectrum rearrangement has been studied in graphene with a binary alloy disorder. Due to limitations in the coherence potential approximation (CPA),[32,36] the results can only appropriately address the electronic structures of graphene with extremely low impurity concentration. In this paper, we propose to calculate the ADOS by the recursion method. Our numerical simulations can provide the accurate ADOS for different impurity concentrations. Moreover, our simulations can also be generalized to study other types of disordered graphene, although the main features of ADOS with a binary alloy disorder in graphene can be characterized by the resonant and antiresonant states caused by the scattering of impurities as reported in Ref. 19. Interestingly, we observe that the impurity concentration (x) and the on-site potential (v) have significant impacts on the main features of ADOS. The impurity concentration shifts the position of resonance energy (E_r). A linear relation for the dip [the minimum in the density of states (DOS)] shift ($\varepsilon_{\text{dip}}=xv$) with a relatively low impurity concentration can be extended to a high impurity concentration case under certain conditions. Moreover, the ADOS with a finite concentration of vacancies is also calculated by using our proposed approach.

This paper is organized as follows: the tight-binding model of graphene with a binary alloy disorder is given in Sec. II. The recursion method is introduced, and its accuracy and applications are also discussed in Sec. II. The ADOS of graphene with different impurity concentrations and on-site potentials is calculated and the detailed discussions are given in Sec. III. Finally, we draw conclusions in Sec. IV.

II. COMPUTATIONAL MODEL AND METHOD

Figure 1 shows the hexagonal lattice structure of a graphene, where each unit cell has two nonequivalent atoms labeled with A and B, respectively. If we consider the contribution from the π bond (one π electron per atom) and the nearest interactions in graphene, the Hamiltonian based on the Wannier representation can be expressed as

$$\hat{H}=\sum_{i}\varepsilon_i|i\rangle\langle i|-t_{ij}\sum_{\langle i,j\rangle}|i\rangle\langle j|, \tag{1}$$

where i and j denote the neighboring sites on the lattice. ε_i is the on-site energy and t_{ij} is the nearest hopping energy (t_{ij}

 ©2008 The American Physical Society

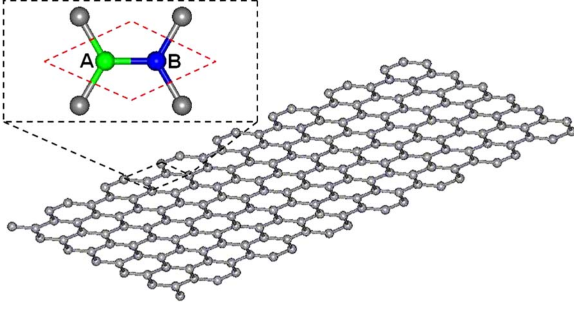

FIG. 1. (Color online) The honeycomb lattice of a graphene. Here, a unit cell is outlined by the red dashed lines, and two non-equivalent atoms are labeled with A (green sphere) and B (blue sphere), respectively.

$=t$ and its value is close to 2.7 eV in graphene). Here, t is scaled to be 1 for simplicity.

With a given impurity concentration (x), the on-site energy ε_i for a binary alloy disordered graphene is equal to v with the probability of x. This model, which is attributed to Lifshitz,[37] features the absolute random distribution of impurities in the space domain. In the following calculations, we focus on studying the properties of the ADOS in two cases. In the first case, the on-site potential (v) varies with given disorder concentrations (x). In the second case, the concentration (x) changes with given on-site potentials (v).

The Lanczos method[38,39] (also called the Haydock–Heine–Kelly recursion method,[40,41] which is a commonly used approach to calculate the ADOS in disorder systems) is adopted in our calculations. The essential idea of the recursion method is that the Hamiltonian matrix is iteratively expressed by using a tridiagonal representation. After selecting a localized seed state ($|f_0\rangle$), this method recursively generates a hierarchy of states ($|f_n\rangle$) based on the defined orthogonal basis as follows:

$$|f_{n+1}\rangle = \hat{H}|f_{n+1}\rangle - \frac{\langle f_n|\hat{H}|f_n\rangle}{\langle f_n|f_n\rangle}|f_n\rangle - \frac{\langle f_n|f_n\rangle}{\langle f_{n-1}|f_{n-1}\rangle}|f_{n-1}\rangle, \quad (2)$$

where, $n=0,1,2,\ldots$, and the recursive coefficients are given by

$$a_n = \frac{\langle f_n|\hat{H}|f_n\rangle}{\langle f_n|f_n\rangle}, b_n = \frac{\langle f_n|f_n\rangle}{\langle f_{n-1}|f_{n-1}\rangle}(b_0=0,|f_{-1}\rangle=0). \quad (3)$$

In the orthogonal basis, the Hamilton matrix becomes

$$H = \begin{pmatrix} a_0 & b_1 & 0 & 0 & \cdots \\ b_1 & a_1 & b_2 & 0 & \cdots \\ 0 & b_2 & a_2 & b_3 & \cdots \\ 0 & 0 & b_3 & a_3 & \cdots \\ \vdots & \vdots & \vdots & \vdots & \ddots \end{pmatrix}. \quad (4)$$

The diagonal elements in Green's function matrix for a seed state can be derived from Eq. (4) based on the continuous-fraction method as follows:

$$G_{00}(E) = \langle f_0|\frac{1}{E-H}|f_0\rangle = \cfrac{1}{E-a_0-\cfrac{b_1^2}{E-a_1-\cfrac{b_2^2}{E-a_2-\cfrac{b_3^2}{\ddots}}}}, \quad (5)$$

and LDOS is defined as

$$\rho_{\text{local}}(E) = \lim_{\varepsilon\to 0^+}\left[-\frac{1}{\pi}G_{00}(E+i\varepsilon)\right]. \quad (6)$$

We can then easily calculate ADOS by using the following equation:

$$\rho_{\text{ave}}(E) = \frac{1}{M}\sum_M \rho_{\text{local}}(E), \quad (7)$$

where M is the number of samples. To terminate continuous fractions, Eq. (5) can be rewritten as

$$G_{00}(E) = \cfrac{1}{E-a_0-\cfrac{b_1^2}{E-a_1-\cfrac{b_2^2}{\cfrac{\cdots}{E-a_n-t(E)}}}}. \quad (8)$$

In Eq. (8), the terminating term can be written as

$$t(E) = \frac{1}{2}\{(E-a_\infty) - [(E-a_\infty)^2 - 4b_\infty^2]^{1/2}\}. \quad (9)$$

The asymptotic value of the continuous-fraction coefficient pairs (a_∞, b_∞) in Eq. (9) can be obtained when n gets large.

This recursion method has been adopted to investigate various disorder systems.[42–44] In fact, an infinite system can be approximated using this method by imposing the periodic boundary condition. The numerical error of DOS is easy to estimate.[43] If the system size (L) and its recursion step (N) are large enough and the corresponding positive broadening width (ε) is reasonably small, the LDOS results should be accurate. It is easy to get a reliable ADOS for a disorder system by averaging over a large number of samples (M). For a perfect graphene, two relations, $\varepsilon \sim 1/L$ and $\rho \sim 1/L$, approximately hold at the Dirac point as shown in Figs. 2(a) and 2(b). Therefore, a large size is needed in simulations to improve the accuracy because the wavelength of the electrons near the Dirac point approaches infinity. As shown in Fig. 2(c), a large recursion step N is also needed to obtain ADOS results with good accuracy (in our simulation, N is set to be $2L$).

The accuracy of the recursion method is examined by comparing the calculated DOSs of a perfect graphene with those obtained based on the strict integral method in the first Brillouin zone (BZ). The calculated DOSs at several energy points are list in Table I. Clearly, the results using the recursion method are highly accurate and their relative errors are very small (<0.002). In the following, we calculate the ADOS of a disordered graphene and the parameters $L=800$, $N=2L$, $\varepsilon=5\times10^{-3}$, and $M=2000$ are chosen.

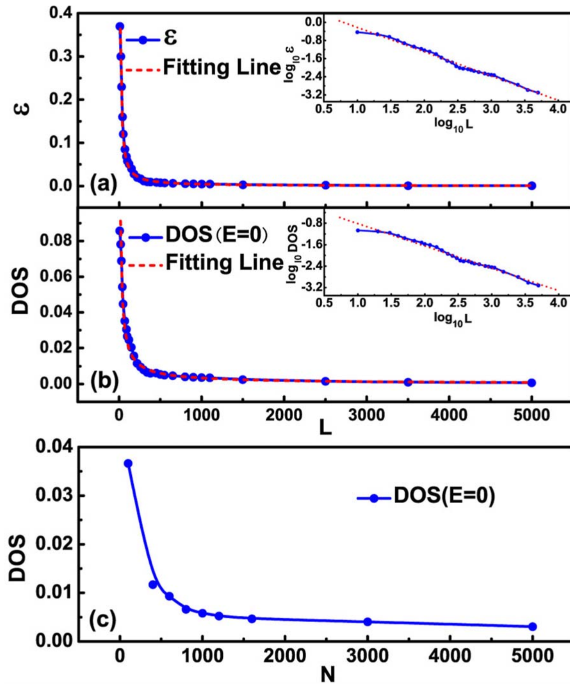

FIG. 2. (Color online) (a) ε and (b) DOS as a function of L (blue solid line) and the corresponding fitting line shown with a red dashed line for a perfect graphene. Insets in (a) and (b) indicate that the relations $\varepsilon \sim 1/L$ and $\rho \sim 1/L$ approximately hold at the Dirac point. (c) DOS (ρ) as a function of N (blue solid line) at the Dirac point ($E=0$). Here, $L=800$.

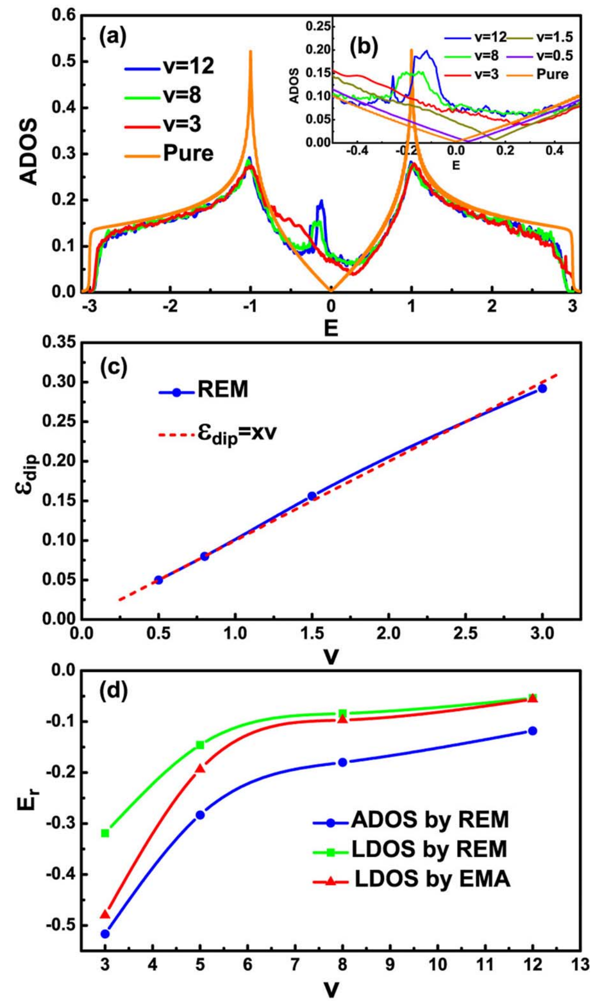

FIG. 3. (Color online) [(a) and (b)] ADOS of a graphene with impurity concentration $x=10\%$ and various on-site potentials (v). (c) The energy shift of the antiresonance state ($\varepsilon_{\mathrm{dip}}$) as a function of the on-site potential (v) (blue solid line). The red dashed line stands for the linear relation $\varepsilon_{\mathrm{dip}}=xv$. (d) The resonance energy (E_r) as a function of the on-site potential (v). The blue, green, and red lines stand for the ADOS of a graphene with $x=10\%$. ADOS is calculated by using the recursion method. LDOS of a single impurity is computed by using the recursion method and EMA.

III. RESULTS AND DISCUSSIONS

Figure 3(a) shows several calculated ADOSs of graphene with a fixed impurity concentration $x=10\%$ but different on-site potentials (v). Our results clearly show that the ADOS remains similar in shape in a high-energy region. However, the ADOS near the Dirac point remarkably changes for different on-site potentials (v). Two striking features are observed. (1) An obvious resonance peak appears in the ADOS curves when $v \geq 3$. Its energy position or the resonance energy (E_r) shifts toward the Dirac point when the on-site potential (v) increases. This peak is attributed to a resonance state. A very similar feature is also observed in the LDOS when there is a single impurity or a low impurity concentration.[30,32] (2) There is a dip (the minimum in the ADOS) near the Dirac point. The position of this dip ($\varepsilon_{\mathrm{dip}}$) shifts with the presence of impurities. As shown in Fig. 3(b), the linear relation, $\varepsilon_{\mathrm{dip}}=xv$, holds when the on-site potential is relatively small, but the dip disappears when v becomes larger (i.e., $v>3$). These results show that the relation ($\varepsilon_{\mathrm{dip}}=xv$) is correct when $v \ll v_{\mathrm{dip}}$, while this relation does not hold for a system with on-site potential $v>v_{\mathrm{dip}}$.

TABLE I. The DOS in a perfect graphene calculated by using both the recursion method and the strict integral method within the first BZ. Here, $L=800$, $N=2L$, and $\varepsilon=5\times10^{-3}$. The relative differences of calculated DOS between two different methods are also listed for clarity.

Energy	0.0	0.4	0.8	1.2	1.6	2.0
The recursion method	0.0037	0.0781	0.1990	0.2570	0.1952	0.1702
The strict integral method	0.0037	0.0781	0.1998	0.2529	0.1938	0.1695
The relative difference	<0.0001	<0.0001	<0.002	<0.002	<0.002	<0.002

To quantitatively explore the impact of the impurity concentration on the shift of resonance energy (E_r), we compare the result of finite impurity concentration with that of a single impurity. The calculated results are shown in Fig. 3(c). Here, we adopt the recursion method and the effective-mass approximation method[45] (EMA) to calculate the position of the resonance energy (E_r) of the LDOS at the impurity site for a single impurity in the graphene system. E_r of finite impurity concentration is determined by using the recursion method.

The Green's function based on the effective-mass approximation in a perfect graphene is expressed as

$$G_0(E) = \lim_{\varepsilon\to 0^+} \frac{S}{\pi}\int_0^{k_c} \frac{(E+i\varepsilon)k}{(E+i\varepsilon)^2+(3tak/2)^2}dk = \frac{\sqrt{3}}{3\pi t^2}E \ln\left|\frac{E^2}{9t^2a^2k_c^2/4-E^2}\right| - i\frac{\sqrt{3}}{3t^2}|E| = \frac{\sqrt{3}}{3\pi}E \ln\left|\frac{E^2}{9a^2k_c^2/4-E^2}\right| - i\frac{\sqrt{3}}{3}|E|, \tag{10}$$

where $S=3\sqrt{3}a^2/2$ is the area of a unit cell in real space, a is a lattice constant, and k_c is the cutoff wave vector and is set to be $2.13/a$.[45] For the simple case, Green's function of a single impurity graphene is expressed as

$$G(E) = \frac{G_0(E)}{1-vG_0(E)} = \left(\frac{\sqrt{3}}{3\pi}E \ln\left|\frac{E^2}{9a^2k_c^2/4-E^2}\right| - \frac{v}{3\pi}E^2 \ln^2\left|\frac{E^2}{9a^2k_c^24-E^2}\right| - \frac{v^2}{3}E^2 - i\frac{\sqrt{3}}{3}|E|\right)\bigg/\left(\left[1-\frac{\sqrt{3}}{3\pi}E \ln\left|\frac{E^2}{9a^2k_c^2/4-E^2}\right|\right]^2+\frac{v^2}{3}E^2\right). \tag{11}$$

LDOS at the impurity site is easy to obtain by

$$\rho_{\mathrm{imp}}(E) = \frac{\sqrt{3}}{3\pi}\frac{|E|}{\left[1-\frac{\sqrt{3}}{3\pi}E \ln\left|\frac{E^2}{9a^2k_c^2/4-E^2}\right|\right]^2+\frac{v^2}{3}E^2}. \tag{12}$$

The resonant energy (E_r) in this case can be defined as

$$1 = v \,\mathrm{Re}\, \mathrm{G}_0(E_r) = \frac{\sqrt{3}v}{3\pi}E_r \ln\left|\frac{E_r^2}{9a^2k_c^2/4-E_r^2}\right|. \tag{13}$$

When the on-site potential (v) increases as shown in Fig. 3(c), E_r shifts toward the Dirac point [Fig. 3(a)]. Due to multiple scattering among impurities, E_r of finite impurity concentration is quite different from that of a single impurity. This observation implies that the multiple scattering processes cannot be neglected for finite concentration cases. Note that the positions of E_r for a single impurity, which are determined by the recursion method and by the effective approximation, are quite different for a relatively small on-site potential and coincide with each other at a large on-site potential. This difference results from the Green's function obtained by Eq. (10), which is valid only in a low-energy region (close to the Dirac point).

Figures 4(a) and 4(b) present the calculated ADOS of a graphene with different impurity concentrations (x) while the on-site potential (v) is set to be 1.5. When the on-site potential (v) is small, the dip exists although the resonance peak is not so obvious. Interestingly, we find that the linear relation $\varepsilon_{\mathrm{dip}}=xv$, as shown in Fig. 4(c), still holds even for a large impurity concentration, considering that the multiple scattering among impurities is strong in this case. The linear relation at a low concentration regime with a small on-site potential can be understood by using a virtual crystal approximation (VCA), which simply predicts the energy level at which two bands are shifted by $\varepsilon_{\mathrm{dip}}=xv$. However, VCA becomes inadequate for the regime of high impurity concentration and large on-site potential. Furthermore, it is

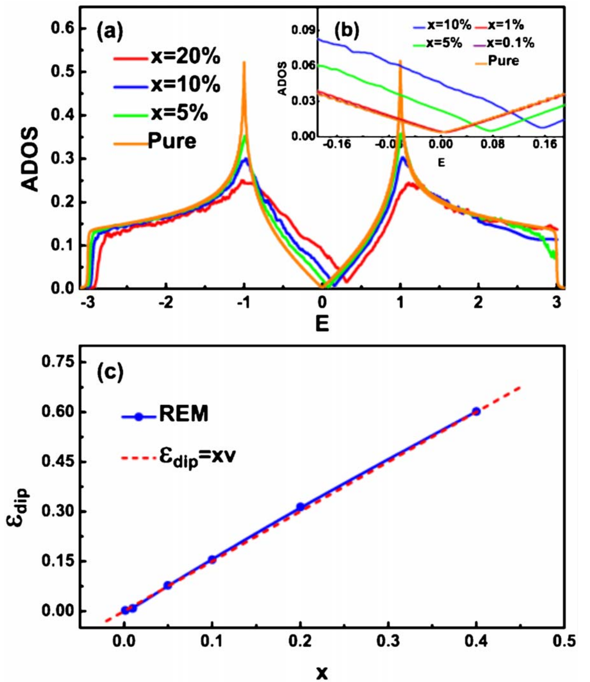

FIG. 4. (Color online) (a) ADOS of a disordered graphene and (b) ADOS near the Dirac point with various impurity concentrations (x). Here, $v=1.5$. (c) The energy shift ($\varepsilon_{\mathrm{dip}}$) as a function of impurity concentrations (x) (blue solid line) for $v=1.5$. The red dashed line shows the following linear relation: $\varepsilon_{\mathrm{dip}}=xv$.

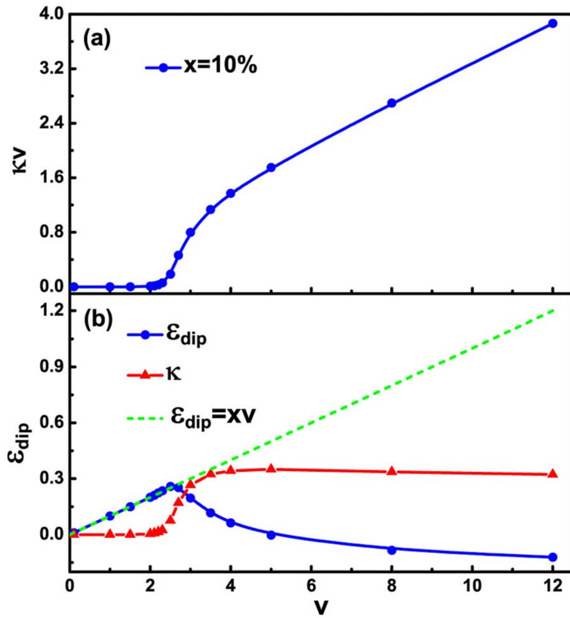

FIG. 5. (Color online) (a) Parameter κv and (b) the energy shift ($\varepsilon_{\rm dip}$) as a function of on-site potential (v), where the impurity concentration is $x=10\%$. The blue and red solid lines stand for the results calculated by using the recursion method and the CPA, respectively. The green dashed line indicates the linear relation $\varepsilon_{\rm dip}=xv$.

also found that the van Hove singularity gradually softens.

To obtain a better understanding of the linear relation $\varepsilon_{\rm dip}=xv$, we present a qualitative discussion based on the CPA. The dip in the LDOS, which indicates the antiresonance states, was approximately investigated based on CPA.[30,32] By ignoring multiple scattering, this method is effective to calculate the dip in the ADOS. Here, the self-energy Σ can be obtained by neglecting multiple scattering processes among the impurities as follows:

$$\Sigma = \frac{xv}{1 - vG_0(E-\Sigma)}. \tag{14}$$

The energy shift $\varepsilon_{\rm dip}$ can be determined by substituting $E-\Sigma=i\kappa$ (here, $\kappa>0$ is real). We can get

$$\varepsilon_{\rm dip} \equiv \mathrm{Re}\,\Sigma = \frac{xv\left(1-\frac{\sqrt{3}\kappa v}{3}\right)}{\left(1-\frac{\sqrt{3}\kappa v}{3}\right)^2 + \frac{1}{3\pi_2}\kappa^2 v^2 \ln^2\left|\frac{\kappa^2}{9a^2k_c^2/4-\kappa^2}\right|}. \tag{15}$$

κ is calculated by the following equation:

$$\mathrm{Im}\,\Sigma = -\kappa = \frac{\frac{\sqrt{3}}{3\pi}\kappa v^2 \ln\left|\frac{\kappa^2}{9a^2k_c^2/4-\kappa^2}\right|}{\left(1-\frac{\sqrt{3}\kappa v}{3}\right)^2 + \frac{1}{3\pi_2}\kappa^2 v^2 \ln^2\left|\frac{\kappa^2}{9a^2k_c^2/4-\kappa^2}\right|}. \tag{16}$$

If $\kappa v \ll 1$, Eq. (15) can be simplified to $\varepsilon_{\rm dip}=xv$. For graphene with a given impurity concentration (e.g., 10%), Fig. 5(a) clearly shows that the value of κv is small when v is less than 2.5. If $\kappa v \ll 1$, the linear relation, $\varepsilon_{\rm dip}=xv$, holds as shown in Fig. 3(b). This observation implies that CPA is a good approximation and the antiresonance states make a great contribution to the ADOS in such a condition. However, the curve of $\varepsilon_{\rm dip}$ as calculated by using the CPA approximation does not match the linear relation ($\varepsilon_{\rm dip}=xv$) when v is larger than 2.5. The possible reason is that multiple scattering among the impurities cannot be neglected in the CPA calculations when $v>2.5$. With the given impurity concentration of 10%, based on the condition of $|\mathrm{Re}\,\Sigma|=|\mathrm{Im}\,\Sigma|$, the threshold value $v_{\rm dip}\approx 2.9$ (estimated by the CPA calculations) of the on-site potential ($v_{\rm dip}$) to preserve the linear relation, which is shown in Fig. 5(b). This result is somewhat underestimated by Fig. 3(a). For instance, the value of $v_{\rm dip}$ should be larger than 3. For the system with a given on-site potential (v), Fig. 6(a) shows that the results by the CPA method are different from those using the recursion method. In the case of $v=1.5$, the inequality $\kappa v \ll 1$ is satisfied only for $x\leq 0.2$. With a small on-site potential, we find that the relation $\varepsilon_{\rm dip}=xv$ still holds even when the impurity concentration is close to 40%. This observation indicates that CPA is not able to obtain a reliable result for graphene when the impurity concentration is large because the approach neglects the important scattering process among impurities.

The threshold impurity concentration ($x_{\rm dip}$) for $v=1.5$ is about 37% according to the linear relationship, as show in Fig. 6(b). When the on-site potential (v) becomes large enough, $x_{\rm dip}$ is extremely small. These results are consistent with results shown in Fig. 5. There is an appreciable dip only for an extremely small impurity concentration. Clearly, $x_{\rm dip}$ is sensitive to the on-site potentials. When the inequality $\kappa v \ll 1$ does not hold anymore, $x_{\rm dip}$ cannot be obtained through simple CPA calculations.[32] Previous theoretical studies[32,36] have suggested that the CPA with single-site scattering may fail to characterize the dip. Our results by the recursion method reveal that the CPA is valid only if ($\kappa v \ll 1$). The linear relation, $\varepsilon_{\rm dip}=xv$, can be further extended to graphene

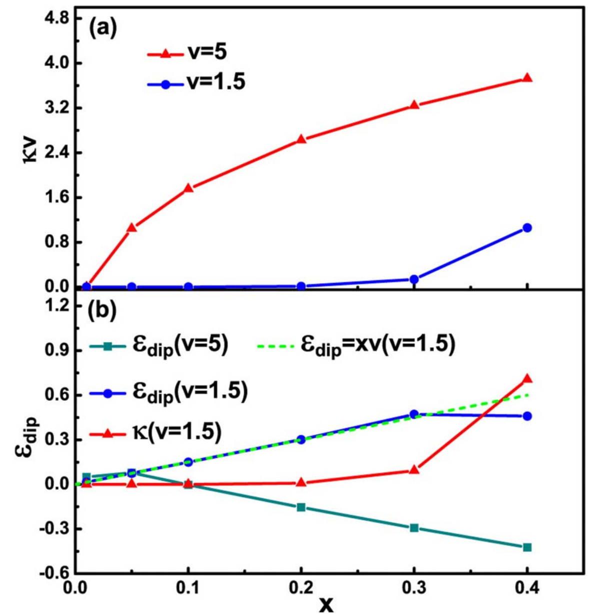

FIG. 6. (Color online) (a) Parameter κv and (b) the energy shift ($\varepsilon_{\rm dip}$) as a function of impurity concentration (x) when $v=1.5$ (blue line) or $v=5$ (dark cyan lines). The red solid line indicates κ as a function of impurity concentration for the $v=1.5$ case. The green dashed line shows the linear relation of $\varepsilon_{\rm dip}=xv$.

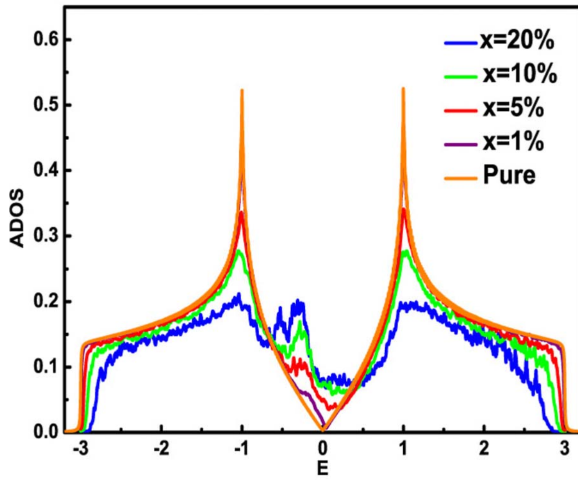

FIG. 7. (Color online) (a) ADOS of a disordered graphene and (b) ADOS near the Dirac point with various impurity concentrations (x). Here, $v=5$.

with high impurity concentrations and small on-site potentials.

For large on-site potentials as shown in Fig. 7, there are distinct resonance peaks. The height of the peak significantly increases as the level of disorder increases. However, the position of the resonance peak shifts little at a high impurity concentration. Generally, E_r is determined by both on-site potential (v) and impurity concentrations (x). However, when the on-site potential is large, E_r does not depend on the impurity concentration even if x has a large value. This might be the consequence of the disappearance of the van Hove singularity when the impurity concentration is about 20%.

The disordered graphene with a finite density of vacancies can be modeled by setting the on-site potential V to a very large value.[34,45] Figure 8 shows the calculated ADOS of graphene systems with vacancies ($V=1000$) based on the recursion method. There is a clear sharp peak near the Dirac point, which is in line with the previously reported numerical results.[35] This sharp peak can be accommodated very well by the Lorentz distribution. However, one theoretical calculation based on the full Born approximation[4] (FBA) predicts that the value of ADOS should exactly be zero. Its error may be due to ignoring multiple scattering in the FBA calculation. In addition, the calculations based on the CPA[4] and the full self-consistent Born approximation[4] (FSBA) fail to produce observable resonance peaks. These inconsistencies indicate the severe limitations of the CPA, FBA, and FSBA methods near the Dirac point, which should be carefully examined further.

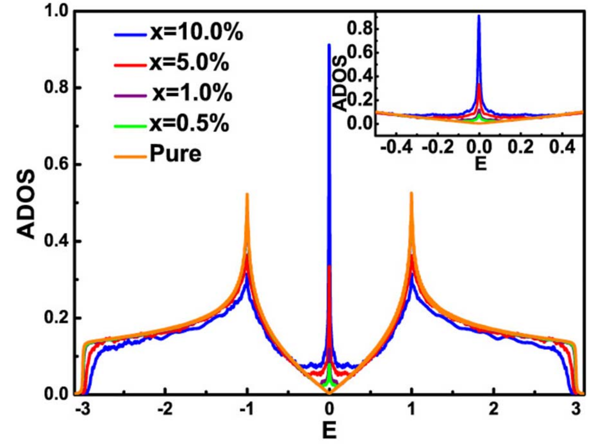

FIG. 8. (Color online) The calculated ADOS of graphene with different concentrations of vacancies. Here, we choose $v=1000$.

IV. CONCLUSION

In this paper, the average density of state in graphene with binary alloy disorders is calculated by using the recursion method. The applicability and accuracy of the recursion method are also addressed. The shape of the resonance peak and the position of the dip are strongly dependent on impurity concentrations (x) and on-site potentials (v). The linear relation, $\varepsilon_{\text{dip}}=xv$, can be derived from the CPA when $\kappa v \ll 1$. This relation can explain the shift of the dip's position at low and high impurity concentrations when the on-site potential is weak. For a large on-site potential, neither CPA nor Eq. (14) works well due to omitting scattering events among impurities, except for an extremely low impurity concentration ($\kappa v \ll 1$). By setting v to be a huge value, we have simulated graphene with a finite concentration of vacancies and observed the resonance peak of ADOS at the Dirac point.

ACKNOWLEDGMENTS

This work was partially supported by the National Natural Science Foundation of China (Grants No. 10574119, No. 20773112, No. 10674121, and No. 50721091), by the National Key Basic Research Program (Grant No. 2006CB922000), and by the Science and Technological Fund of Anhui Province for Outstanding Youth. J.C. would like to acknowledge the funding support from the Discovery program of the Natural Sciences and Engineering Research Council of Canada under Grant No. 245680 and support from the National Science Council. Work at NTU is supported in part by COE-SUG (Grant No. M58070001) and A*STAR SERC (Grant No. 0521170032).

*Corresponding author; phsqw@ustc.edu.cn

[1] K. S. Novoselov, A. K. Geim, S. V. Morozov, D. Jiang, Y. Zhang, S. V. Dubonos, I. V. Grigorieva, and A. A. Firsov, Science **306**, 666 (2004).
[2] K. S. Novoselov, A. K. Geim, S. V. Morozov, D. Jiang, M. I. Katsnelson, I. V. Grigorieva, S. V. Dubonos, and A. A. Firsov, Nature (London) **438**, 197 (2005).
[3] Y. B. Zhang, Y. W. Tan, Horst L. Stormer, and Philip Kim, Nature (London) **438**, 201 (2005).
[4] N. M. R. Peres, F. Guinea, and A. H. Castro Neto, Phys. Rev. B

73, 125411(2006).
[5] M. I. Katsnelson, Eur. Phys. J. B **51**, 157 (2006).
[6] J. Cserti, Phys. Rev. B **75**, 033405 (2007).
[7] K. Ziegler, Phys. Rev. Lett. **97**, 266802 (2006).
[8] V. P. Gusynin and S. G. Sharapov, Phys. Rev. B **73**, 245411 (2006).
[9] K. Ziegler, Phys. Rev. B **75**, 233407 (2007).
[10] K. Nomura and A. H. MacDonald, Phys. Rev. Lett. **98**, 076602 (2007).
[11] K. Han, D. Spemann, P. Esquinazi, R. Höhne, R. Riede, and T. Butz, Adv. Mater. (Weinheim, Ger.) **15**, 1719 (2003).
[12] M. A. H. Vozmediano, M. P. López-Sancho, T. Stauber, and F. Guinea, Phys. Rev. B **72**, 155121 (2005).
[13] R. Tamura and M. Tsukada, Phys. Rev. B **55**, 4991 (1997).
[14] T. Nakanishi and T. Ando, J. Phys. Soc. Jpn. **66**, 2973 (1997).
[15] Y. Kopelevich, P. Esquinazi, J. Torres, and S. Moehlecke, J. Low Temp. Phys. **119**, 691 (2000).
[16] F. Schedin, A. K. Geim, S. V. Morozov, D. Jiang, E. H. Hill, P. Blake, and K. S. Novoselov, Nat. Mater. **6**, 652 (2007).
[17] A. A. Ovchinnikov and I. L. Shamovsky, J. Mol. Struct.: THEOCHEM **251**, 133 (1991).
[18] J. González, F. Guinea, and M. A. H. Vozmediano, Phys. Rev. Lett. **69**, 172 (1992).
[19] J. C. Charlier, T. W. Ebbesen, and Ph. Lambin, Phys. Rev. B **53**, 11108 (1996).
[20] K. Wakabayashi and M. Sigrist, Phys. Rev. Lett. **84**, 3390 (2000).
[21] K. Wakabayashi, Phys. Rev. B **64**, 125428 (2001).
[22] J. González, F. Guinea, and M. A. H. Vozmediano, Phys. Rev. B **63**, 134421 (2001).
[23] K. Harigaya, J. Phys.: Condens. Matter **13**, 1295 (2001).
[24] H. Matsumura and T. Ando, J. Phys. Soc. Jpn. **70**, 2657 (2001).
[25] K. Harigaya, A. Yamashiro, Y. Shimoi, K. Wakabayashi, Y. Kobayashi, N. Kawatsu, K. Takai, H. Sato, J. Ravier, T. Enoki, and M. Endo, J. Phys. Chem. Solids **65**, 123 (2004).
[26] E. J. Duplock, M. Scheffler, and P. J. D. Lindan, Phys. Rev. Lett. **92**, 225502 (2004).
[27] P. O. Lehtinen, A. S. Foster, Yuchen Ma, A. V. Krasheninnikov, and R. M. Nieminen, Phys. Rev. Lett. **93**, 187202 (2004).
[28] W. M. Hu, J. D. Dow, and C. W. Myles, Phys. Rev. B **30**, 1720 (1984).
[29] A. Lherbier, Blanca Biel, Y. Niquet, and S. Roche, Phys. Rev. Lett. **100**, 036803 (2008).
[30] Y. V. Skrypnyk and V. M. Loktev, Phys. Rev. B **73**, 241402(R) (2006).
[31] Y. V. Skrypnyk and V. M. Loktev, Low Temp. Phys. **33**, 762 (2007).
[32] Y. V. Skrypnyk and V. M. Loktev, Phys. Rev. B **75**, 245401 (2007).
[33] Y. G. Pogorelov, arXiv:cond-mat/0603327 (unpublished).
[34] T. O. Wehling, A. V. Balatsky, M. I. Katsnelson, A. I. Lichtenstein, K. Scharnberg, and R. Wiesendanger, Phys. Rev. B **75**, 125425 (2007).
[35] V. M. Pereira, F. Guinea, J. M. B. Lopes dos Santos, N. M. R. Peres, and A. H. Castro Neto, Phys. Rev. Lett. **96**, 036801 (2006).
[36] Y. V. Skrypnyk, Phys. Rev. B **70**, 212201 (2004).
[37] I. M. Lifshitz, Adv. Phys. **13**, 483 (1964).
[38] C. Lanczos, J. Res. Natl. Bur. Stand. **45**, 255 (1950).
[39] G. Grosso and G. P. Parravicini, *Solid State Physics* (Elsevier, Singapore, 2006).
[40] R. Haydock, V. Heine, and M. J. Kelly, J. Phys. C **5**, 2845 (1972).
[41] R. Haydock, V. Heine, and M. J. Kelly, J. Phys. C **8**, 2591 (1975).
[42] J. J. Sinai, C. Wongtawatnugool, and S. Y. Wu, Phys. Rev. B **26**, 1829 (1982).
[43] R. Haydock and R. L. Te, Phys. Rev. B **49**, 10845 (1994).
[44] D. J. Lohrmann, L. Resca, G. P. Parravicini, and R. D. Graft, Phys. Rev. B **40**, 8404 (1989).
[45] Z. F. Wang, Ruoxi Xiang Q. W. Shi, Jinlong Yang, Xiaoping Wang, J. G. Hou, and Jie Chen, Phys. Rev. B **74**, 125417 (2006).